



Overexpressing IFITM family genes predict poor prognosis in kidney renal clear cell carcinoma

Ying Xu^{1,2#}, Danqi Huang^{3#}, Kun Zhang², Zengqi Tang³, Jianchi Ma³, Mansheng Zhu⁴, Hui Xiong^{2,3}

¹Department of Clinical Laboratory, Sun Yat-sen Memorial Hospital, Sun Yat-sen University, Guangzhou, China; ²Guangdong Provincial Key Laboratory of Malignant Tumor Epigenetics and Gene Regulation, Sun Yat-sen Memorial Hospital, Sun Yat-sen University, Guangzhou, China; ³Department of Dermatology, Sun Yat-sen Memorial Hospital, Sun Yat-sen University, Guangzhou, China; ⁴Department of General Surgery, Nanfang Hospital, Southern Medical University, Guangzhou, China

Contributions: (I) Conception and design: None; (II) Administrative support: None; (III) Provision of study materials or patients: None; (IV) Collection and assembly of data: None; (V) Data analysis and interpretation: Y Xu, M Zhu; (VI) Manuscript writing: All authors; (VII) Final approval of manuscript: All authors.

[#]These authors contributed equally to this work.

Correspondence to: Mansheng Zhu; Hui Xiong. Department of Dermatology, Sun Yat-sen Memorial Hospital, Sun Yat-sen University, Guangzhou, China. Email: mansheng_zhu@163.com; xiongh9@mail.sysu.edu.cn.

Background: The interferon-inducible transmembrane (IFITM) proteins are localized in the endolysosomal and plasma membranes, conferring cellular immunity to various infections. However, the relationship with carcinogenesis remains poorly elucidated. In the present study, we investigated the role of IFITM in kidney renal clear cell carcinoma (KIRC).

Methods: We utilized the online databases of OncoPrint, UALCAN and Human Protein Atlas to analyze the expression of IFITMs and validate their levels in human KIRC cells by qPCR and western blot. Furthermore, we evaluated prognostic significance with the Gene Expression Profiling Interactive Analysis tool (Kaplan-Meier (KM) Plotter) and delineated the immune cell infiltration profile related to IFITMs with the TIMER2.0 database.

Results: IFITMs were overexpressed in KIRC and varied in subtypes and tumor grades. High expression of IFITMs indicated a poor prognosis and more immune cell infiltration, especially endothelial cells and cancer-associated fibroblasts. IFITMs were associated with immune genes, which correlated with poor prognosis of renal clear cell carcinoma. We also explored the enriched network of IFITMs co-occurrence genes and their targeted transcription factors and miRNA. The expression of IFITMs correlated with hub mutated genes of KIRC.

Conclusions: IFITMs play a crucial role in the oncogenesis of KIRC and could be a potential surrogate marker for treatment response to targeted therapies.

Keywords: Interferon-induced transmembrane proteins (IFITM); kidney renal clear cell carcinoma (KIRC); prognosis; tumor infiltration

Submitted Sep 18, 2021. Accepted for publication Oct 21, 2021.

doi: 10.21037/tau-21-848

View this article at: <https://dx.doi.org/10.21037/tau-21-848>

Introduction

Renal cell cancer (RCC) is the most prevalent form of kidney cancer and is notorious for its metastatic potential (1). According to the pathological classification by the International Society of Urological Pathology Vancouver

Consensus Statement, RCC is categorized into clear cell, and types I and II papillary and chromophobe subtypes (2). Clear cell RCC or kidney renal clear cell carcinoma (KIRC), accounting for 75% of RCC cases, is one of the most aggressive (3).

Table 1 Sequence of gene-specific primers for qPCR.

Gene	Forward sequence (5'- 3')	Reverse sequence (5'- 3')
<i>IFITM-1</i>	GGCTTCATAGCATTTCGCCTACTC	AGATGTTTCAGGCACTTGGCGGT
<i>IFITM-2</i>	CATCCCGGTAACCCGATCAC	CACGGAGTACGCGAATGCTA
<i>IFITM-3</i>	CATCCAGTAACCCGACCG	TGTTGAACAGGGACCAGACG
<i>GAPDH</i>	GGAGCGAGATCCCTCCAAAAT	GGCTGTTGTCATACTTCTCATGG

KIRC stands out as one of the most immune infiltrated tumors in pan-cancer comparisons (4). Recently immune checkpoint inhibitors (ICIs) have proven highly efficacious in this disease (5). Tumor microenvironment (TME) heavily impacts KIRC cell biology and affects tumor prognosis and treatment response (4). Tumor-infiltrating cells of TME could demonstrate either tumor-suppressive or tumor-promoting effects, depending on distinct tumor models (6). Unlike most other cancer types, overall high CD8 T cell infiltration in KIRC was associated with worse prognosis (7). So, it is important to clarify the heterogeneous tumor microenvironment of KIRC.

Interferon-induced transmembrane proteins (IFITMs) are reported to be interacted with immune cell infiltration (8). IFITMs are a family of effector proteins that impede pathogenic virus entry into host cells. IFITM-1, IFITM-2 and IFITM-3 are the most common isoforms. IFITM-1 is mainly located on the cytoplasmic membrane for entry prevention of the virus, while IFITM-2 and IFITM-3 localize to the endosomal compartment to block fusion pore formation. IFITMs markedly enhance the antiviral activity of monoclonal antibodies against hepatitis C virus and thus might prevent the development of hepatocellular carcinoma (9). IFITM-3 was discovered to be a prognostic indicator for acute myeloid leukemia (10). Also, IFITM2 has been demonstrated to promote gastric cancer progression by promoting cell migration, invasion, and inducing EMT in GC cells (11). However, the role of IFITMs in KIRC and the interactions of IFITMs with TME have been rarely reported and await further clarification. In the present study, we investigated the role of IFITMs in KIRC. Various bioinformatics tools were utilized to investigate their potential biological functions, prognostic values, and regulatory network, as well as the effect on immune cell infiltration. The results of this study provide preliminary evidence of the oncogenic effect, and interacting relationships of IFITMs. We present the following article in accordance with the REMARK

reporting checklist (available at <https://dx.doi.org/10.21037/tau-21-848>).

Methods

Cell cultures

The KIRC cell line (Caki-1) and normal kidney cell line (HK-2) were kindly donated by Dr. Zhiliang Chen. Caki-1 cells were cultured in McCoy's 5a Modified Medium (Boster, China) and HK-2 was maintained in Dulbecco's Modified Eagle Medium/Nutrient Mixture F-12 (Gibco). Both media contained 1% penicillin and streptomycin (HyClone), as well as 10% fetal bovine serum (FBS, Gemini). All cells were cultured in a humidified 5% CO₂ environment at 37 °C.

Quantitative reverse transcription polymerase chain reaction (qRT-PCR)

Total RNA was extracted from cells using the EZ-press RNA Purification Kit (EZBioscience, Guangzhou, China). The RNA purity was evaluated by A260:A280 ratio using a NanoDrop spectrophotometer (ND-2000c). cDNA was synthesized using the PrimeScript RT Reagent Kit (Takara, Japan). qRT-PCR was completed on a LightCycler 480 (Roche), using TB Green Premix Ex Taq (Takara Bio). Denaturation was set at 95 °C for 30 s with 40 total cycles and a second step at 95 °C for 5 s. The expression levels of genes were normalized to that of GAPDH and determined by the Ct^{-ΔΔt} method. Gene-specific primers were listed in the *Table 1*.

Western blot

Cells were lysed with buffer (CWbio, China) on ice, and proteins (20 mg) were separated on 10% sodium dodecyl sulfate/polyacrylamide gel electrophoresis gel (Beyotime, China), before being transferred to polyvinylidene

difluoride membranes (Millipore, Burlington, MA, USA). Membranes were blocked by 5% bovine serum albumin (MRC, China) for 1 h at room temperature and then incubated with IFITM-1/-2/-3 antibody (1:1,000, Santa Cruz Biotechnology, CA, USA) or GAPDH (1:8,000, Cell Signaling Technology) overnight at 4 °C. After washing three times with TBST, membranes were blocked with horseradish peroxidase conjugated secondary antibodies (CWbio, China). Subsequently, protein expression was examined by a G: BOX ChemiXT4 Imaging System (Bio-Rad) with an enhanced chemiluminescence kit (Merck Millipore, Germany).

Oncomine analysis

Oncomine (www.oncomine.org) is a comprehensive resource for counting gene expression signatures, clusters and gene-set modules (12). We used the Oncomine dataset to analyze the mRNA expression level in various cancer and related normal tissues. A P value cutoff was set at 0.001, and the log-fold change threshold was set at 2. The gene rank threshold was defined as the top 10%. The study was conducted in accordance with the Declaration of Helsinki (as revised in 2013).

Expression Atlas analysis

The expression of IFITMs in the KIRC cell line was analyzed by Expression Atlas (13) (<https://www.ebi.ac.uk/gxa/home>). The expression level in TPM (Transcript per million, TPM) was set at 0.5.

Human Protein Atlas analysis

The immunohistochemical profiles of normal kidney tissue and KIRC were derived from the Human Protein (14) Atlas (<https://www.proteinatlas.org/>). The antibodies used for IFITM-1 (<https://www.proteinatlas.org/ENSG00000185885-IFITM1/pathology/renal+cancer#ihc>), IFITM-2 (<https://www.proteinatlas.org/ENSG00000185201-IFITM2/pathology/renal+cancer>), and IFITM-3 (<https://www.proteinatlas.org/ENSG00000142089-IFITM3/pathology/renal+cancer>) were HPA004810, HPA004337, and HPA004337 respectively. Clinical information of the patients can be obtained from the website.

UALCAN database analysis

The UALCAN database (15) is a comprehensive web

resource for studying cancer data (<http://ualcan.path.uab.edu/index.html>). We used it to evaluate the expression of IFITMs in KIRC based on different subtypes.

TISIDB database analysis

The TISIDB database (<http://cis.hku.hk/TISIDB/index.php>) is a valuable resource for cancer immunology research and therapy (16). We used it to analyze the expression of IFITMs in KIRC based on different grades and immune subtypes. We also explored the correlation between IFITMs and immune genes.

Kaplan-Meier survival analysis

We used KM Plotter for the survival analysis (17) to assess the effect of IFITMs and related immune genes on survival of KIRC (<https://kmplot.com/analysis/index.php?p=background>). The samples were split into high and low expression groups by the best cutoff value of mRNA expression of IFITMs.

TIMER2.0 database analysis

The TIMER2.0 database (<http://timer.cistrome.org/>) (18) is a web-based tool for systematic analysis of immune infiltrates across various cancer types. We explored the association between levels of IFITM gene expressions (log₂ TPM), the abundance of infiltrating immune cells and the clinical relevance. Tumor purity was used for P value correction.

LinkedOmics analysis

The LinkedOmics database (19) (<http://www.linkedomics.org/login.php>) is a cancer-associated multi-dimensional dataset. We chose the RNAseq data type, HiSeq RNA platform and Pearson's correlation coefficient for analysis. We then used the LinkInterpreter module to perform gene set enrichment analysis (GSEA) analysis, which included gene ontology (GO) analysis, Kyoto Encyclopedia Genes and Genomes (KEGG) pathway, kinase target, miRNA target and transcription target. The minimum number of genes (size) was set at 3 and simulations were set at 500.

Database for annotation, visualization, and integrated discovery database analysis

The top 50 co-expressing co-occurrence genes with IFITMs were obtained from cBioPortal (20) (<https://www.cbioportal.com>).

Table 2 Transcription levels of IFITMs in KIRC compared with normal kidney in different studies

Gene	Fold change	P value	t-test	Ref
IFITM-1	2.608	1.12E-04	9.735	Higgins <i>et al.</i> , 2003 (24)
	2.125	4.14E-05	5.229	Lenburg <i>et al.</i> , 2003 (25)
	2.293	2.31E-06	6.531	Gumz <i>et al.</i> , 2007 (26)
	2.227	1.13E-11	8.983	Jones <i>et al.</i> , 2005 (27)
IFITM-2	2.436	5.78E-04	9.329	Higgins <i>et al.</i> , 2003 (24)
	1.921	3.41E-04	4.221	Lenburg <i>et al.</i> , 2003 (25)
	3.168	8.84E-08	8.442	Gumz <i>et al.</i> , 2007 (26)
	1.836	2.87E-05	6.831	Yusenko <i>et al.</i> , 2009 (28)
IFITM-3	1.748	1.34E-06	7.174	Lenburg <i>et al.</i> , 2003 (25)
	2.603	2.43E-08	9.263	Gumz <i>et al.</i> , 2007 (26)
	1.779	4.59E-05	7.178	Yusenko <i>et al.</i> , 2009 (28)

IFITM, interferon-inducible transmembrane; KIRC, kidney renal clear cell carcinoma.

org/) for functional enrichment analysis. These three gene lists were put into Metascape (21) (<https://metascape.org/gp/index.html#/main/step1>) to draw a protein-protein interaction (PPI) network and into Network Analyst (22) (<https://www.networkanalyst.ca/>) for transcription factor-gene interactions and gene-miRNA interactions analyses.

TCGA portal

We obtained the relevance between IFITM mRNA expressions and the mutation rate of 9 hub genes in KIRC from the TCGA portal (23) (<http://tcgportal.org/index.html>).

Statistical analysis

All statistical analyses were performed using SPSS 20.0 software (IBM, USA). Two-tailed Student's *t*-tests were used for comparisons between groups. One-way ANOVA with Bonferroni's test was utilized for multiple comparisons. A two-sided P value <0.05 was considered statistically significant.

Results

Expression levels of IFITM family genes in KIRC

From the Oncomine database, we discovered that the expression levels of IFITMs were higher in cancerous

tissues than in normal tissues for various types of malignancies, but especially kidney cancer (*Figure 1A*; specific data are shown in *Table 2*). The expression profile in KIRC was quite unanimous among IFITM-1, IFITM-2 and IFITM-3, suggesting an important relationship between IFITM and KIRC. Different KIRC cell lines also confirmed the significantly higher expression of these three genes than in normal renal epithelial cells (*Figure 1B*). As for the translational level, the Human Protein Atlas demonstrated positive expression of IFITM using immunohistochemistry (*Figure 1C*). We validated the higher expression of IFITM-1/-2/-3 in the KIRC cell line than in the normal kidney cell line by qPCR (*Figure 1D*) and western blot (*Figure 1E*).

Clinical significance of IFITM in RCC

KIRC can be further subdivided into two subtypes, ccA and ccB, which are characterized by excessive angiogenesis and better prognosis, and by abundant macrophage infiltration and worse prognosis, respectively. From the UALCAN database, these subtypes exhibited a high level of IFITM family expression (*Figure 2A*). Moreover, the expression of the three IFITM members positively correlated with tumor grade (*Figure 2B*). By applying the Kaplan-Meier method, we found that each of the FITM isoform negatively correlated with overall survival in KIRC patients (*Figure 2C*). And the diagnostic role of IFITMs in KIRC

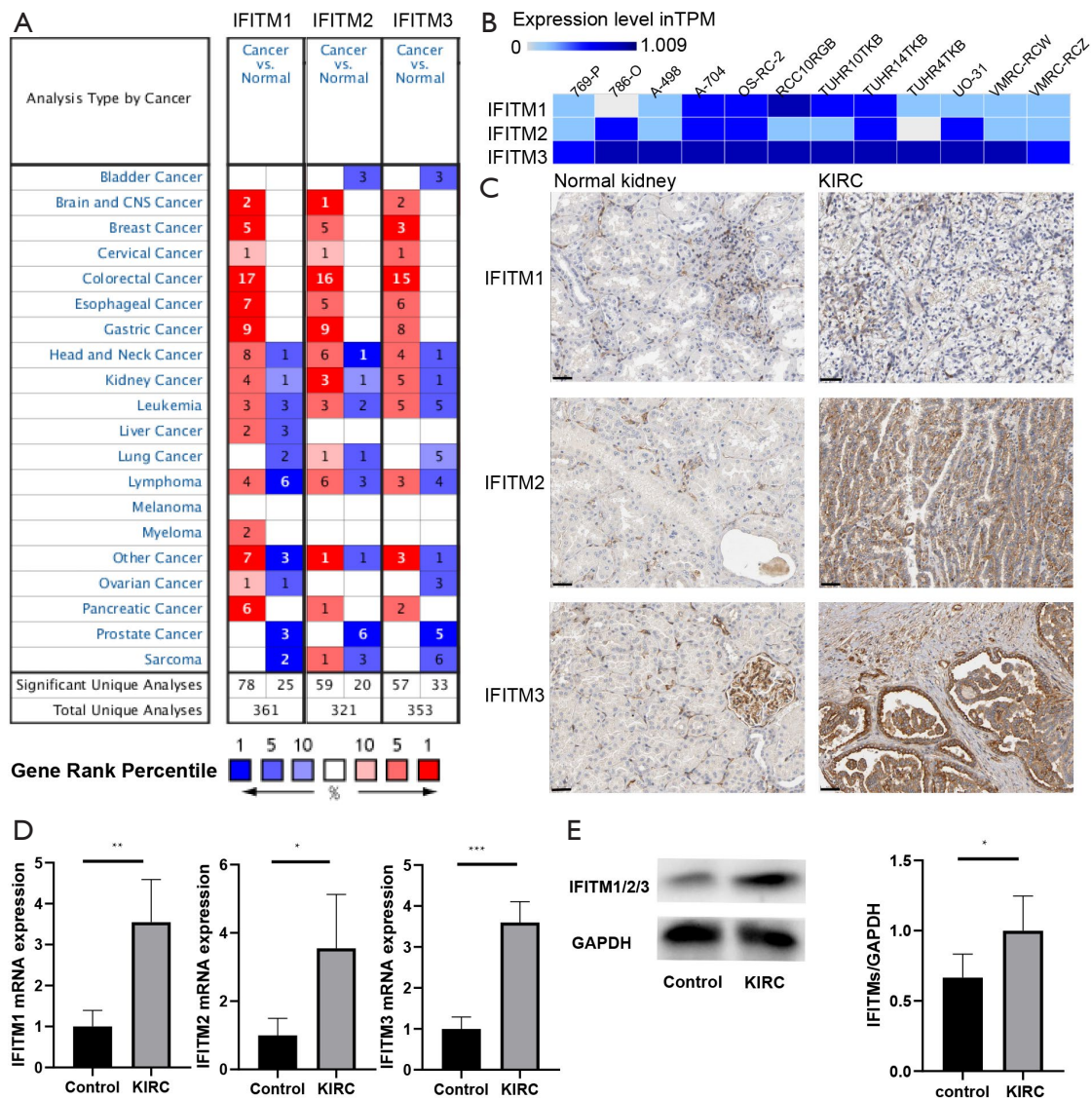


Figure 1 Upregulated expression levels of IFITM family genes in KIRC. (A) mRNA expression levels of IFITMs (cancer compared with normal tissue) analyzed by the OncoPrint database. The graphic shows the numbers of datasets with statistically significant mRNA overexpression (red) or underexpression (blue) of the target genes. (B) Expression of IFITMs in different KIRC cell lines (Expression Atlas data). (C) Protein expression of IFITMs in KIRC and normal kidney tissue assessed by IHC (Human Protein Atlas data), Scale bars: 50 μ m. (D-E) Expression levels of IFITMs human KIRC cell line (Caki-2) and normal kidney cell line (HK-2) validated by qPCR (D) and western blot (E). *, $P < 0.05$; **, $P < 0.01$; ***, $P < 0.001$. IFITM, interferon-inducible transmembrane; KIRC, kidney renal clear cell carcinoma.

was assessed by receiver operating characteristic (ROC) curve analysis (based on TCGA normal kidney samples and KIRC samples). The area under the ROC curve (AUC) analysis displayed that each of the IFITM isoform (IFITM1, IFITM2 and IFITM3) was sensitive and specific for the diagnosis of KIRC (AUC = 0.7721, 0.7280, 0.8292, respectively) (Figure 2D).

Correlation of IFITMs with immune infiltrates in KIRC

For the different immune subtypes, the expression level of the IFITM family was lowest in the immunologically quiet subtype and highest in the tumor growth factor (TGF)- β dominant subtype (Figure 3A). The correlations between the IFITMs and the immune genes are listed in Table 3. The

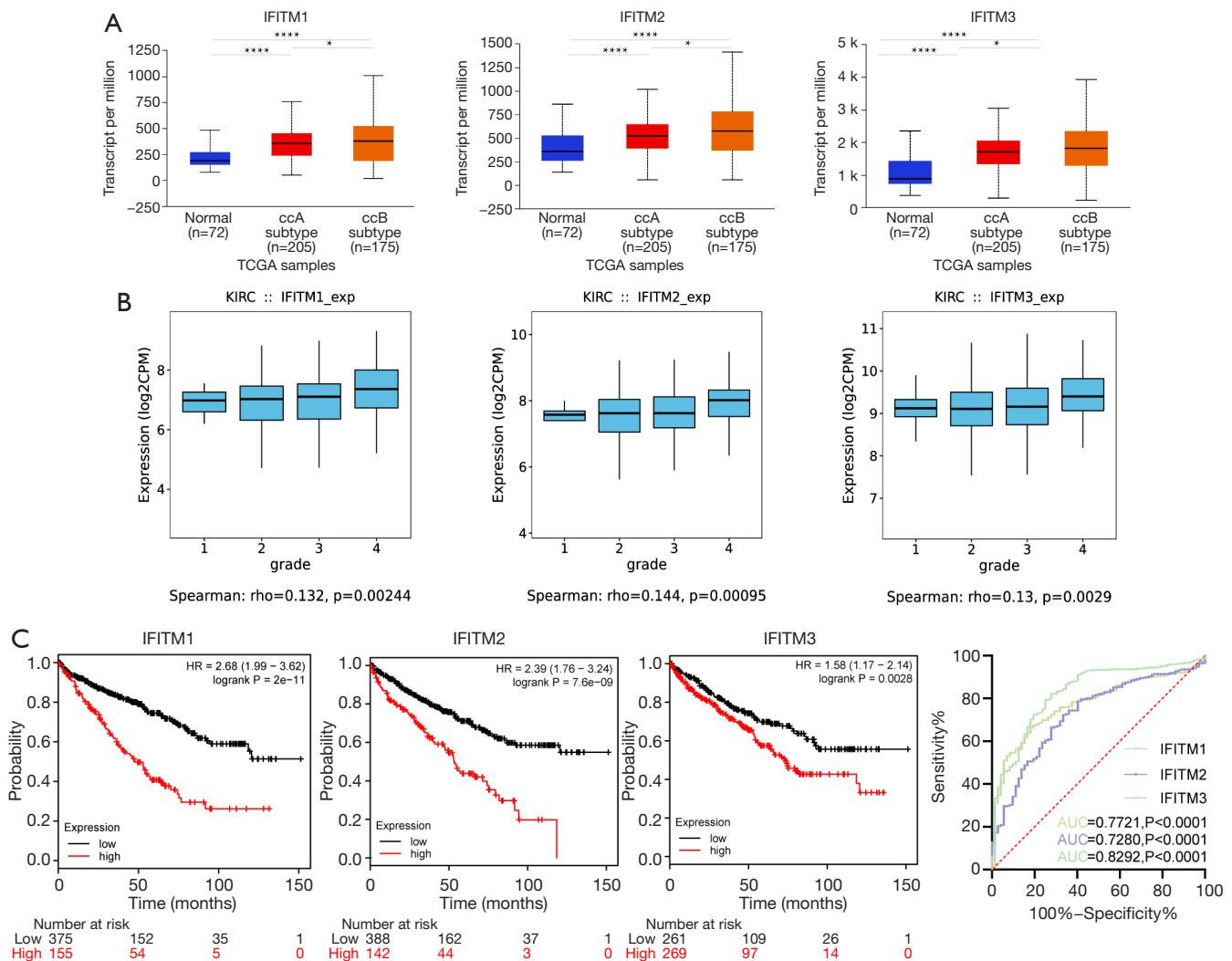


Figure 2 Clinical significance of IFITM in KIRC. (A,B) Relative mRNA expression of IFITM-1, -2 and -3 in normal individuals or KIRC patients with different (A) subtypes (UALCAN database) and (B) grade (TISIDB database). (C) Overall survival of KIRC patients with low/high expression of IFITM family members (KM Plotter). (D) Diagnostic role of IFITMs in KIRC assessed by ROC curve analysis (based on TCGA normal kidney samples and KIRC samples). *, P<0.05; ****, P<0.0001. IFITM, interferon-inducible transmembrane; KIRC, kidney renal clear cell carcinoma. ROC, receiver operating characteristic.

TIMER2.0 database was used to analyze the relationships between the IFITM family and TIL in KIRC. It showed that cancer associated fibroblasts (CAFs), endothelial cells (ECs), myeloid cells, dendritic cells and natural killer (NK) cell infiltrations significantly correlated with the expression of IFITM-1, -2 and -3 (Figure 3B). CAFs and ECs were further analyzed for their role in survival. Notably, the infiltration of CAFs was significant for survival only when IFITMs expression was low, whereas an abundance of ECs positively correlated with KIRC survival irrespective of the expression level of IFITMs (Figure 3C).

GSEA and regulation network of IFITMs in KIRC

GSEA delineated the enrichment profile of IFITMs in KIRC, showing that biological processes such as the response to type I interferon, extracellular structure organization and vasculogenesis were significantly enriched in the GO analysis (Figure 4A), whereas NK cell cytotoxicity, ribosome activity and cytokine-cytokine receptor interaction were enriched in the KEGG analysis (Figure 4B). Furthermore, cBioPortal provided a series of genes that co-expressed with IFITMs, with which we were able to develop a PPI network (Figure 5A).

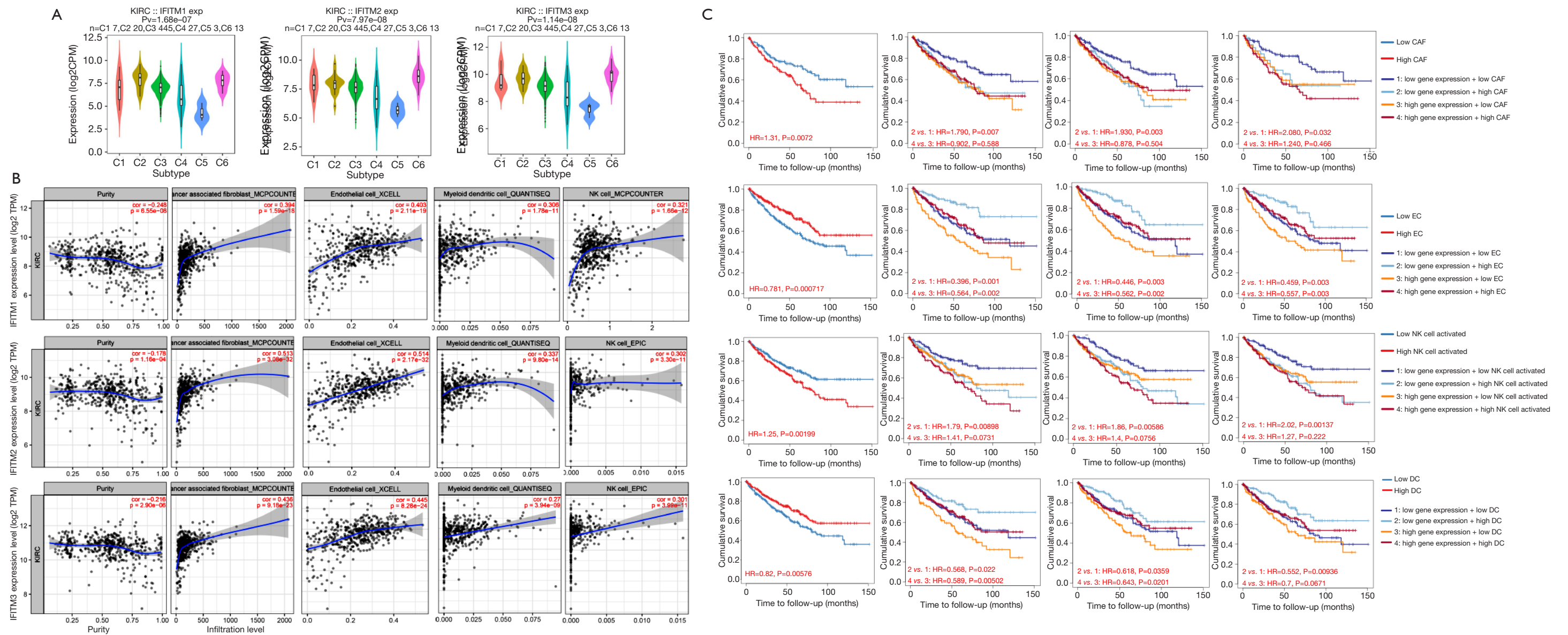


Figure 3 Relation of IFITM expressions to immune cell infiltration. (A) IFITM expressions were least abundant in C5 (immunologically quiet) immune subtype. C1 (wound healing); C2 (interferon-gamma dominant); C3 (inflammatory); C4 (lymphocyte depleted); C5 (immunologically quiet); C6 (TGF- β dominant) (TISIDB database). (B) IFITM expressions positively correlate with infiltration of immune cells including cancer-associated fibroblasts (CAFs), endothelial cells (EC), myeloid dendritic cells and NK cells (Timer). (C) Overall survival analysis of KIRC patients with different IFITM expression levels and infiltration of CAFs, EC, and myeloid-derived suppressor cells (Timer). IFITM, interferon-inducible transmembrane; KIRC, kidney renal clear cell carcinoma.

Table 3 Correlation of immune-related genes with IFITM expressions and effect on prognosis of KIRC

Immune genes	Spearman rho			Overall survival in KIRC	
	IFITM-1	IFITM-2	IFITM-3	HR	Log-rank P
Immunoinhibitors					
<i>TGFB1</i>	0.499	0.526	0.505	1.67 (1.23–2.27)	0.00092
<i>LGALS9</i>	0.485	0.387	0.446	1.96 (1.45–2.65)	6.90E-06
<i>ADORA2A</i>	0.448	0.283	0.337	0.7 (0.52–0.94)	0.017
Immunostimulators					
<i>TNFRSF4</i>	0.486	0.553	0.534	0.75 (0.54–1.04)	0.083
<i>TNFRSF8</i>	0.476	0.401	0.422	1.64 (1.21–2.22)	0.0012
<i>TNFRSF17</i>	0.443	0.448	0.382	1.54 (1.12–2.11)	0.0075
<i>TNFRSF18</i>	0.472	0.4	0.465	0.45 (0.34–0.61)	9.20E-08
<i>CXCR4</i>	0.469	0.447	0.417	1.67 (1.24–2.26)	0.00068
Chemokines					
<i>CCL5</i>	0.434	0.264	0.364	0.57 (0.42–0.78)	0.00038
Receptors					
<i>CCR10</i>	0.432	0.469	0.446	1.55 (1.13–2.12)	0.006

Data from TISIDB and KM Plotter. HR, Hazard Ratio; IFITM, interferon-inducible transmembrane; KIRC, kidney renal clear cell carcinoma.

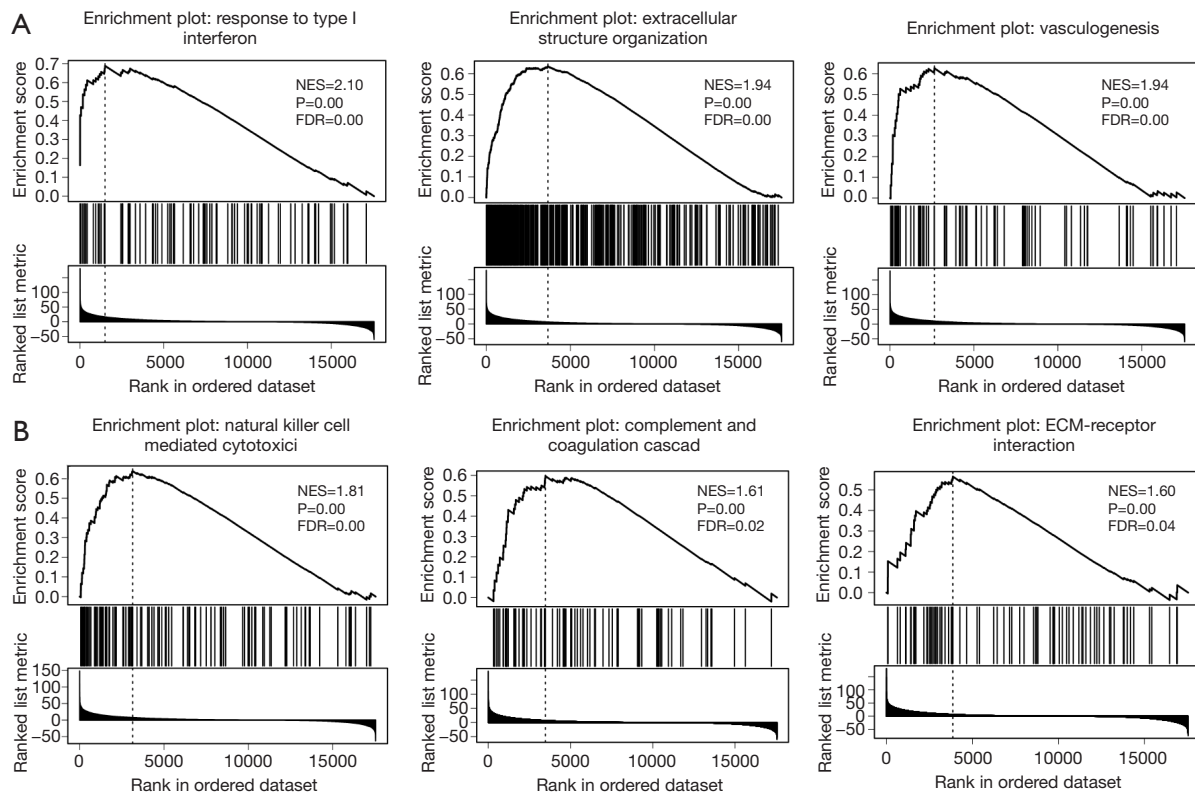


Figure 4 Significantly enriched GO biological process annotations and KEGG pathways of IFITMs in KIRC. (A) Significantly enriched GO biological process annotations analyzed by GSEA (Linkedomics database). (B) KEGG pathways of enriched IFITMs genes in KIRC assessed by GSEA analysis (Linkedomics database). IFITM, interferon-inducible transmembrane; KIRC, kidney renal clear cell carcinoma. GO, gene ontology; GSEA; gene set enrichment analysis.

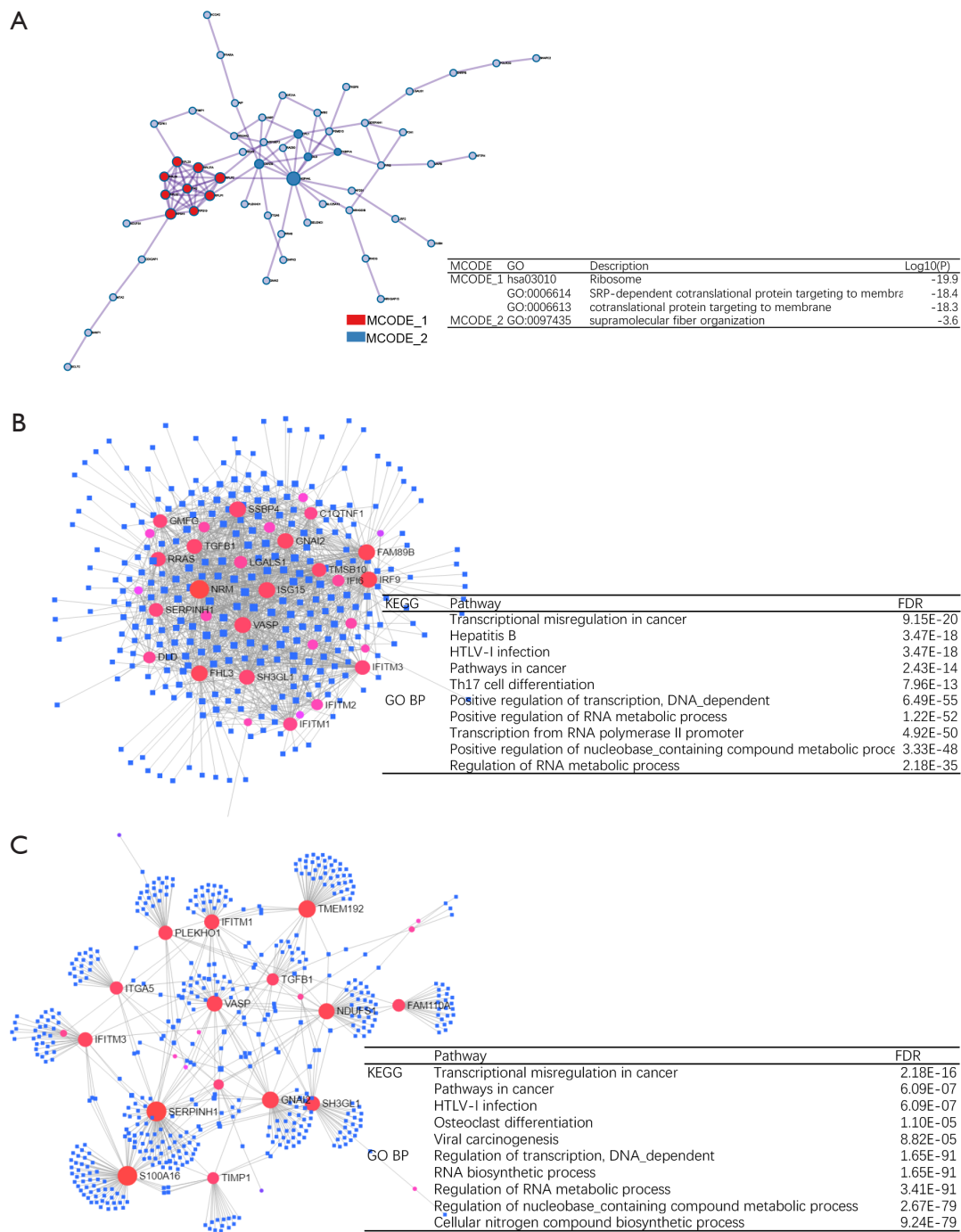


Figure 5 Interaction network of IFITMs co-occurrence genes. (A) The protein-protein interaction (PPI) network (Metascape database). (B) The transcription factor-gene interactions (NetworkAnalyst). (C) The gene-miRNA interactions (NetworkAnalyst).

To explore the upstream regulation relationship of IFITMs, we utilized the ChIP-seq data from the ENCODE database to define the transcription factor-gene interactions (Figure 5B). The

miRNA-gene interactions of IFITMs and the co-expressing genes were also analyzed using TarBase and miRTarBase (Figure 5C). As can be seen in Table 4, the putative miRNAs that

Table 4 Kinases, miRNAs and transcription factor targets of IFITMs in KIRC

Gene	Enriched category	Gene set	Leading edge number	P value	FDR
<i>IFITM-1</i>	miRNA target	GGGGCCC, MIR-296	34	0	0.012
		ATCATGA, MIR-433	25	0	0.101
		ATGTTAA, MIR-302C	65	0	0.141
		TAATGTG, MIR-323	59	0	0.171
		CCAGGGG, MIR-331	32	0.005	0.173
	Kinase target	Kinase_LCK	24	0	0
	Transcription factor	V\$CREL_01	97	0	0.001
		V\$IRF7_01	102	0	0.002
		V\$NERF_Q2	106	0	0.002
		V\$ELF1_Q6	99	0	0.002
		V\$SRF_Q6	86	0	0.003
<i>IFITM-2</i>	miRNA target	TAATGTG, MIR-323	53	0	0
		ATCATGA, MIR-433	40	0	0
		ATGTTAA, MIR-302C	87	0	0
		ATTACAT, MIR-380-3P	25	0	0.009
		TACAATC, MIR-508	21	0	0.011
	Kinase target	Kinase_PAK1	17	0	0.005
	Transcription factor	V \$ STAT5B_01	70	0	0.002
		V \$ SRF_Q5_01	77	0	0.002
		V \$ LFA1_Q6	78	0	0.003
		GGGNNTTCC_V \$ NFKB_Q6_01	46	0	0.003
		V \$ SP1_Q6_01	65	0	0.004
<i>IFITM-3</i>	miRNA target	TGAATGT, MIR-181A, MIR-181B, MIR-181C, MIR-181D	176	0	0
		ATTACAT, MIR-380-3P	29	0	0
		TAATGTG, MIR-323	68	0	0
		ATCATGA, MIR-433	40	0	0
		ATGTTAA, MIR-302C	78	0	0
	Kinase target	CATTTC, MIR-203	88	0	0.001
		Kinase_PAK1	50	0	0
	Transcription factor	Kinase_IKBKB	28	0	0.024
		V \$ SP1_Q6_01	72	0	0.004
		GGGNNTTCC_V \$ NFKB_Q6_01	54	0	0.004
		V \$ LFA1_Q6	79	0	0.004
V \$ STAT5B_01		82	0	0.004	
V \$ NERF_Q2	73	0	0.004		

Data from LinkedOmics. IFITM, interferon-inducible transmembrane; KIRC, kidney renal clear cell carcinoma; FDR, false discovery rate.

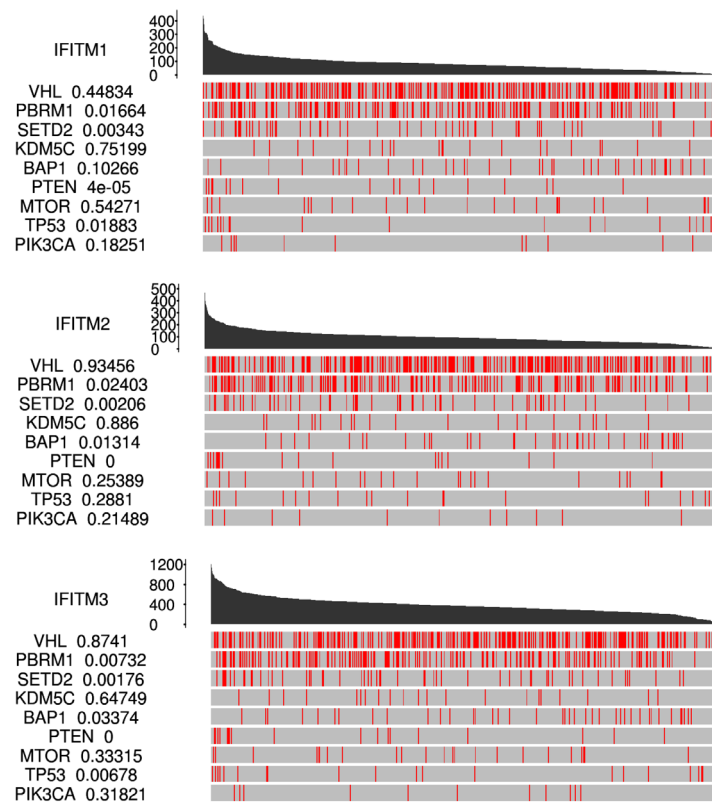


Figure 6 Relevance between IFITMs mRNA expression and the mutation rate of 9 hub genes in KIRC. The right panel is the permutation test P value of expression FPKM between driver mutated (red) and non-mutated (gray) samples. IFITM, interferon-inducible transmembrane; KIRC, kidney renal clear cell carcinoma.

bound to the 3'-UTR of IFITMs were miR-433, miR-302c and miR-323.

Correlation of the expression of IFITMs with significantly mutated genes in KIRC

Nine hub genes have found to be related to KIRC, including *VHL*, *PBRM1*, and *SETD2*. As the IFITM1–3 mRNA expression increased, the mutation rate of *PBRM1*, *SETD2* and *PTEN* mRNA increased. As the IFITM-1 and IFITM-3 mRNA expression increased, the mutation rate of *TP53* mRNA increased (Figure 6).

Discussion

IFITMs, initially identified as interferon-stimulated genes (ISGs), are a family of small homologous proteins that confer restrictions on viral entry (29). Recent discoveries demonstrated that IFITMs are expressed in human lymphocytes and influence T cell differentiation and are

involved in cytokine signaling regulation (30). Because IFITMs are transcriptional targets of Wnt and Hedgehog signaling (31,32), it is possible that they also play an essential role in carcinogenesis. Indeed, the IFITM family is a prognostic indicator for colorectal cancer, gallbladder cancer and acute myeloid leukemia (10,31,33). Their effect on KIRC, however, is seldom discussed.

In this study, we utilized TCGA data and multiple online analysis tools to delineate the role of IFITMs in KIRC and found that IFITM proteins 1, 2 and 3 were all overexpressed in cancerous tissues compared with adjacent normal tissues at both the transcriptional and translational level. Kaplan-Meier analysis showed that higher expression of IFITMs was associated with a worse prognosis. Moreover, enrichment analysis demonstrated that biological processes such as the response to type I interferon, extracellular structure organization and carcinogenesis were highly enriched in the GO analysis. In contrast, NK cell cytotoxicity, ribosome activity and cytokine-cytokine receptor interaction were enriched in the KEGG analysis.

The regulation network was further established based on the miRNA-mRNA and PPI interaction prediction tools. As a result, we found that miR-433, miR-302c and miR-323 possessed a putative binding sequence to the 3'-UTR of IFITMs. For an evaluation of protein interaction, interferon regulatory factor 9 (IRF9) and interferon alpha inducible protein 6 (IFI6) were predicted to be targets of IFITMs. IRF9 is a transcription factor that mediates type I IFN signaling, leading to tyrosine phosphorylation of STAT1 and STAT2, thus activating the JAK/STAT pathway (34). IFI6 is also induced by interferon and regulates tumor cell apoptosis (35). Together with IFITMs, IRF9 and IFI6 might constitute part of the innate immune response against KIRC. Sure enough, the host immunity toward KIRC was quite active according to our findings from the immune cell infiltration analysis, in which myeloid cells, dendritic cells and NK cell infiltrations significantly correlated with the expression of IFITMs. Cytokine-cytokine receptor interaction and JAK/STAT pathway activation by IFITMs and its targets might be contributed to recruit immune cell infiltration into tumor microenvironment of KIRC.

As for the different immune subtypes, the expression of IFITMs was markedly lower in the immunologically quiet subtype and higher in the TGF- β dominant subtype, indicating that the level of IFITMs might represent the level of immune activity. As a common sense, more immune cell infiltration was beneficial for prognosis. But in the present study, we found that high expression of IFITMs indicated a poor prognosis and more immune cell infiltration. It might be on this account that tumor-infiltrating cells acted a multifaceted role (tumor-suppressive or tumor-enhanced effects) depending on the different cancer types (6). Unlike most other cancer types, high CD8 T cell infiltration in KIRC predicted poor outcomes. The CD8 TILs were found to be abundant in KIRC, but they were functionally and metabolically impaired, and lost tumor-killing activities, thereby suppressed its antitumor immunity in KIRC (7).

Targeted therapies directed against VEGFR and mammalian target of rapamycin (mTOR) were approved for RCC as early as 2005 (36). These regimens were developed based on the observation that *VHL* was often altered in sporadic RCC (37). Although these regimens were designated to address altered *VHL* biology, treatment response was not dependent on the absence or presence of *VHL* alterations (38). Biomarkers for treatment response were later revealed, as the alterations in chromatin-remodeling genes such as *PBRM1*, *BAP1*, *SETD2* and *EZH2* were found to be closely associated with clinical

outcomes (39-42). Among them, *PBRM1*, *BAP1* and *SETD2* are all localized in close proximity on the short arm of chromosome 3. *PBRM1* is the major component of the PBAF (Polybromo-associated BAF) complex. Although *PBRM1* has been reported to be a tumor suppressor in KIRC by regulating cellular proliferation and differentiation, the mutation of this gene is the second most common somatic alteration in KIRC and is detected in $\approx 30\%$ of patients (43,44). The loss of *PBRM1* might upregulate HIF and STAT3 and thus strengthen immune surveillance against cancer (45). *SETD2* is a histone H3 K36 methyltransferase that modulates chromatin biology and regulates gene transcription and DNA repair. Mutation of *SETD2* invariably coexists with mutation of *PBRM1* (46). Evidence revealed that the level of mutation positively correlates with stages of the disease, suggesting a preventive role against tumor metastasis of the wild-type *SETD2* (47). *BAP1* is a two-hit tumor suppressor gene. Unlike *SETD2*, the simultaneous loss of both *BAP1* and *PBRM1* is seen in only 3% of cases (48). In addition, there is almost no overlap between the gene signatures of *BAP1* and *PBRM1* mutation, suggesting a mutually exclusive oncogenic mechanism (40). According to our correlation analysis of IFITM expressions and gene mutations, the mutations of *PBRM1*, *BAP1* and *SETD2* were all significantly correlated with the three IFITM genes' expression. These results further suggested that IFITMs might play a crucial role in the oncogenesis of KIRC and could be a potential surrogate marker for treatment response to targeted therapies.

We have several limitations to our study. Firstly, the oncogenic role and regulation interaction networks of IFITM have yet to be validated by additional cellular and animal experiments in further study. Additionally, correlation analysis between the expression of IFITMs and the treatment response to targeted therapies is warranted with real-world data.

Conclusions

The discoveries in our study help our understanding of the role of IFITMs in the oncogenesis of KIRC and suggest avenues for further research on new diagnostic and therapeutic targets of KIRC.

Acknowledgments

Funding: This work was supported by grants from the Natural Science Foundation of Guangdong Province

(2020A1515010115), the Fundamental Research Funds for the Central University (20ykpy109, 19ykpy103).

Footnote

Reporting Checklist: The authors have completed the REMARK reporting checklist. Available at <https://dx.doi.org/10.21037/tau-21-848>

Data Sharing Statement: Available at <https://dx.doi.org/10.21037/tau-21-848>

Conflicts of Interest: All authors have completed the ICMJE uniform disclosure form (available at <https://dx.doi.org/10.21037/tau-21-848>). All authors reported that this work was supported by grants from the Natural Science Foundation of Guangdong Province (2020A1515010115) and the Fundamental Research Funds for the Central University (20ykpy109, 19ykpy103). The authors have no other conflicts of interest to declare.

Ethical Statement: The authors are accountable for all aspects of the work in ensuring that questions related to the accuracy or integrity of any part of the work are appropriately investigated and resolved. The study was conducted in accordance with the Declaration of Helsinki (as revised in 2013).

Open Access Statement: This is an Open Access article distributed in accordance with the Creative Commons Attribution-NonCommercial-NoDerivs 4.0 International License (CC BY-NC-ND 4.0), which permits the non-commercial replication and distribution of the article with the strict proviso that no changes or edits are made and the original work is properly cited (including links to both the formal publication through the relevant DOI and the license). See: <https://creativecommons.org/licenses/by-nc-nd/4.0/>.

References

1. Barata PC, Rini BI. Treatment of renal cell carcinoma: Current status and future directions. *CA Cancer J Clin* 2017;67:507-24.
2. Srigley JR, Delahunt B, Eble JN, et al. The International Society of Urological Pathology (ISUP) Vancouver Classification of Renal Neoplasia. *Am J Surg Pathol* 2013;37:1469-89.
3. Hsieh JJ, Le VH, Oyama T, et al. Chromosome 3p Loss-Orchestrated VHL, HIF, and Epigenetic Deregulation in Clear Cell Renal Cell Carcinoma. *J Clin Oncol* 2018. [Epub ahead of print]. doi: 10.1200/JCO.2018.79.2549.
4. Vuong L, Kotecha RR, Voss MH, et al. Tumor Microenvironment Dynamics in Clear-Cell Renal Cell Carcinoma. *Cancer Discov* 2019;9:1349-57.
5. Motzer RJ, Tannir NM, McDermott DF, et al. Nivolumab plus Ipilimumab versus Sunitinib in Advanced Renal-Cell Carcinoma. *N Engl J Med* 2018;378:1277-90.
6. Şenbabaoğlu Y, Gejman RS, Winer AG, et al. Tumor immune microenvironment characterization in clear cell renal cell carcinoma identifies prognostic and immunotherapeutically relevant messenger RNA signatures. *Genome Biol* 2016;17:231.
7. Siska PJ, Beckermann KE, Mason FM, et al. Mitochondrial dysregulation and glycolytic insufficiency functionally impair CD8 T cells infiltrating human renal cell carcinoma. *JCI Insight* 2017;2:e93411.
8. Diamond MS, Farzan M. The broad-spectrum antiviral functions of IFIT and IFITM proteins. *Nat Rev Immunol* 2013;13:46-57.
9. Wrensch F, Ligat G, Heydmann L, et al. Interferon-Induced Transmembrane Proteins Mediate Viral Evasion in Acute and Chronic Hepatitis C Virus Infection. *Hepatology* 2019;70:1506-20.
10. Liu Y, Lu R, Cui W, et al. High IFITM3 expression predicts adverse prognosis in acute myeloid leukemia. *Cancer Gene Ther* 2020;27:38-44.
11. Xu L, Zhou R, Yuan L, et al. IGF1/IGF1R/STAT3 signaling-inducible IFITM2 promotes gastric cancer growth and metastasis. *Cancer Lett* 2017;393:76-85.
12. Rhodes DR, Kalyana-Sundaram S, Mahavisno V, et al. OncoPrint 3.0: genes, pathways, and networks in a collection of 18,000 cancer gene expression profiles. *Neoplasia* 2007;9:166-80.
13. Papatheodorou I, Fonseca NA, Keays M, et al. Expression Atlas: gene and protein expression across multiple studies and organisms. *Nucleic Acids Res* 2018;46:D246-51.
14. Uhlen M, Zhang C, Lee S, et al. A pathology atlas of the human cancer transcriptome. *Science* 2017;357:eaan2507.
15. Chandrashekar DS, Bashel B, Balasubramanya SAH, et al. UALCAN: A Portal for Facilitating Tumor Subgroup Gene Expression and Survival Analyses. *Neoplasia* 2017;19:649-58.
16. Ru B, Wong CN, Tong Y, et al. TISIDB: an integrated repository portal for tumor-immune system interactions. *Bioinformatics* 2019;35:4200-2.
17. Nagy Á, Lániczky A, Menyhart O, et al. Validation of

- miRNA prognostic power in hepatocellular carcinoma using expression data of independent datasets. *Sci Rep* 2018;8:9227.
18. Li T, Fu J, Zeng Z, et al. TIMER2.0 for analysis of tumor-infiltrating immune cells. *Nucleic Acids Res* 2020;48:W509-14.
 19. Vasaikar SV, Straub P, Wang J, et al. LinkedOmics: analyzing multi-omics data within and across 32 cancer types. *Nucleic Acids Res* 2018;46:D956-63.
 20. Cerami E, Gao J, Dogrusoz U, et al. The cBio cancer genomics portal: an open platform for exploring multidimensional cancer genomics data. *Cancer Discov* 2012;2:401-4.
 21. Zhou Y, Zhou B, Pache L, et al. Metascape provides a biologist-oriented resource for the analysis of systems-level datasets. *Nat Commun* 2019;10:1523.
 22. Zhou G, Soufan O, Ewald J, et al. NetworkAnalyst 3.0: a visual analytics platform for comprehensive gene expression profiling and meta-analysis. *Nucleic Acids Res* 2019;47:W234-41.
 23. Xu S, Feng Y, Zhao S. Proteins with Evolutionarily Hypervariable Domains are Associated with Immune Response and Better Survival of Basal-like Breast Cancer Patients. *Comput Struct Biotechnol J* 2019;17:430-40.
 24. Higgins JP, Shinghal R, Gill H, et al. Gene expression patterns in renal cell carcinoma assessed by complementary DNA microarray. *Am J Pathol* 2003;162:925-32.
 25. Lenburg ME, Liou LS, Gerry NP, et al. Previously unidentified changes in renal cell carcinoma gene expression identified by parametric analysis of microarray data. *BMC Cancer* 2003;3:31.
 26. Gumz ML, Zou H, Kreinest PA, et al. Secreted frizzled-related protein 1 loss contributes to tumor phenotype of clear cell renal cell carcinoma. *Clin Cancer Res* 2007;13:4740-9.
 27. Jones J, Otu H, Spentzos D, et al. Gene signatures of progression and metastasis in renal cell cancer. *Clin Cancer Res* 2005;11:5730-9.
 28. Yusenkov MV, Zubakov D, Kovacs G. Gene expression profiling of chromophobe renal cell carcinomas and renal oncocytomas by Affymetrix GeneChip using pooled and individual tumours. *Int J Biol Sci* 2009;5:517-27.
 29. Brass AL, Huang IC, Benita Y, et al. The IFITM proteins mediate cellular resistance to influenza A H1N1 virus, West Nile virus, and dengue virus. *Cell* 2009;139:1243-54.
 30. Yáñez DC, Sahni H, Ross S, et al. IFITM proteins drive type 2 T helper cell differentiation and exacerbate allergic airway inflammation. *Eur J Immunol* 2019;49:66-78.
 31. Andreu P, Colnot S, Godard C, et al. Identification of the IFITM family as a new molecular marker in human colorectal tumors. *Cancer Res* 2006;66:1949-55.
 32. Furmanski AL, Barbarulo A, Solanki A, et al. The transcriptional activator Gli2 modulates T-cell receptor signalling through attenuation of AP-1 and NFκB activity. *J Cell Sci* 2015;128:2085-95.
 33. Li D, Yang Z, Liu Z, et al. DDR2 and IFITM1 Are Prognostic Markers in Gallbladder Squamous Cell/ Adenosquamous Carcinomas and Adenocarcinomas. *Pathol Oncol Res* 2019;25:157-67.
 34. Fink K, Martin L, Mukawera E, et al. IFNβ/TNFα synergism induces a non-canonical STAT2/IRF9-dependent pathway triggering a novel DUOX2 NADPH oxidase-mediated airway antiviral response. *Cell Res* 2013;23:673-90.
 35. Qadir F, Aziz MA, Sari CP, et al. Transcriptome reprogramming by cancer exosomes: identification of novel molecular targets in matrix and immune modulation. *Mol Cancer* 2018;17:97.
 36. Rini BI, Small EJ. Biology and clinical development of vascular endothelial growth factor-targeted therapy in renal cell carcinoma. *J Clin Oncol* 2005;23:1028-43.
 37. Garcia JA, Rini BI. Recent progress in the management of advanced renal cell carcinoma. *CA Cancer J Clin* 2007;57:112-25.
 38. Ricketts CJ, De Cubas AA, Fan H, et al. The Cancer Genome Atlas Comprehensive Molecular Characterization of Renal Cell Carcinoma. *Cell Rep* 2018;23:313-326.e5.
 39. Ho TH, Choueiri TK, Wang K, et al. Correlation Between Molecular Subclassifications of Clear Cell Renal Cell Carcinoma and Targeted Therapy Response. *Eur Urol Focus* 2016;2:204-9.
 40. Peña-Llopis S, Vega-Rubín-de-Celis S, Liao A, et al. BAP1 loss defines a new class of renal cell carcinoma. *Nat Genet* 2012;44:751-9.
 41. Sato Y, Yoshizato T, Shiraishi Y, et al. Integrated molecular analysis of clear-cell renal cell carcinoma. *Nat Genet* 2013;45:860-7.
 42. Adelaiye-Ogala R, Budka J, Damayanti NP, et al. EZH2 Modifies Sunitinib Resistance in Renal Cell Carcinoma by Kinome Reprogramming. *Cancer Res* 2017;77:6651-66.
 43. Varela I, Tarpey P, Raine K, et al. Exome sequencing identifies frequent mutation of the SWI/SNF complex gene PBRM1 in renal carcinoma. *Nature* 2011;469:539-42.
 44. Hodges C, Kirkland JG, Crabtree GR. The Many Roles of BAF (mSWI/SNF) and PBAF Complexes in Cancer. *Cold Spring Harb Perspect Med* 2016;6:a026930.

45. Nargund AM, Pham CG, Dong Y, et al. The SWI/SNF Protein PBRM1 Restrains VHL-Loss-Driven Clear Cell Renal Cell Carcinoma. *Cell Rep* 2017;18:2893-906.
46. Peña-Llopis S, Christie A, Xie XJ, et al. Cooperation and antagonism among cancer genes: the renal cancer paradigm. *Cancer Res* 2013;73:4173-9.
47. Hsieh JJ, Chen D, Wang PI, et al. Genomic Biomarkers of a Randomized Trial Comparing First-line Everolimus and Sunitinib in Patients with Metastatic Renal Cell Carcinoma. *Eur Urol* 2017;71:405-14.
48. Joseph RW, Kapur P, Serie DJ, et al. Clear Cell Renal Cell Carcinoma Subtypes Identified by BAP1 and PBRM1 Expression. *J Urol* 2016;195:180-7.

Cite this article as: Xu Y, Huang D, Zhang K, Tang Z, Ma J, Zhu M, Xiong H. Overexpressing IFITM family genes predict poor prognosis in kidney renal clear cell carcinoma. *Transl Androl Urol* 2021;10(10):3837-3851. doi: 10.21037/tau-21-848